Vibroacoustic Effects in MEMS

Roman Vinokur, Wieland Associates Inc., Laguna Hills, California

The invention of the transistor started a microelectronic revolution. While integrated circuit (IC) microtechnology provided high-speed and low-cost signal processing capabilities, conventional transducers (sensors and actuators) remained far behind in size and cost. The Micro Electro Mechanical System (MEMS) technology arose to create relatively cheap transducers, compatible in size with their IC controllers, to meet the needs of medicine, aviation, the automotive industry, military applications and security. One challenge is that phenomena ignored on the macro scale become important at the microscopic level. In particular, vibration effects in electrostatic sensors and actuators cannot be fully interpreted using classical engineering models with linear springs, insignificant air damping, etc. Non-linearity, instability, potentially high air damping, molecular slip flow, and Coulomb interaction must be considered to design robust MEMS transducers. Although some conceptions were developed even before the MEMS era (in particular for condenser microphones[1]), they remain little-known to most engineers. This article describes important vibroacoustic effects in electrostatic (capacitive) microsensors.

MEMS technology combines micromachining with microelectronics – the next logical step in the silicon revolution – and is very promising for aerospace, automotive, biological/medical, military, and photonics applications. The term MEMS came into existence in the late 1980s although 'bulk' and 'surface' micromachining were developed earlier. A typical MEMS design incorporates at least one of the following components: a microsensor (accelerometer, load cell, microphone, etc.), microactuator (lever, gear, micro-mirror, valve, pump, motor, etc.), processor chip, and package. The size of microtransducers (microsensors and microactuators) is commonly measured in millimeters or even microns. While small size may be very important, for many mechanical systems miniaturization is not practical and the primary reason for MEMS is their low cost per device. The package shields the device from unfavorable thermal, vibration, acoustics, stress/strain, and electromagnetic effects, and connects it to the outside electrical circuits and mechanical mountings. During the last decade, silicon microtechnology produced a variety of sensors for measuring position, velocity, acceleration, pressure, sound pressure, force, torque, angle rate, flow, magnetic field, temperature, gas composition, humidity, pH, gas/liquid molecular concentrations, etc. To some extent, the contemporary MEMS products may be compared with Thomas Edison's incandescent bulb that glowed dim and yellowish because the carbon-type filament turned to ashes with temperature. Only upon the implementation of tungsten filaments many years later did electric light bulbs become really luminous and robust. Currently, many of the MEMS designs described in publications are prototypes rather than robust industrial products. The reason is not just a deficit of optimal materials (like tungsten for Edison's bulbs). Laboratory techniques, poor manufacturing bases, and organizational and financial pitfalls have been factors. It is likely that a lack of sufficient practical experience and theoretical knowledge has also contributed.

Capacitive Parallel-Plate Sensor

The conventional electrostatic parallel-plate model of a capacitive sensor includes: a linear spring, dashpot and parallel-plate capacitor – one of the plates playing the role of a mechanical mass. It was first developed, utilizing electroacoustics, for electrostatic transducers (microphones and speakers)[1] and later rediscovered for MEMS applications.[2] As shown in Figure 1, the bottom plate is fixed and the downward direction is considered positive.

The upper plate movement is governed by the differential equation

$$M\frac{d^2Y(t)}{dt^2} + K(1+i\eta)Y(t) - \frac{\varepsilon\,A\,U^2}{2\,[d-Y(t)]^2} = F_{\text{ext}}(t) \qquad (1)$$

inertial force
elastic and friction force
electrostatic force
external force (pressure, gravity, etc.)

where:
$Y(t)$ = displacement of the upper plate ($0 \le Y \le d$)
M = mass of the upper plate
K = mechanical spring constant
η = loss factor
d = gap between the parallel plates under static equilibrium at zero voltage and external force
A = area of each plate
U = voltage applied to the capacitor
ε = permittivity of a vacuum – approximately equal to the permittivity of air, $\varepsilon \approx 8.854(pF/m)$

The total loss factor η is a sum of several components determined by various energy dissipation mechanisms: (1) viscous friction in the air gap; (2) hysteresis or structural loss in the spring element; and (3) sound radiation by the moving mass into the ambient air (this effect is commonly minor in comparison to the viscous friction). For sensors, voltage U = const. The magnitude of the electrical charge on each plate can be expressed as

$$Q(t) = \frac{\varepsilon AU}{d - Y(t)}$$

and the upper plate's displacement can be detected through measuring the capacitor's electrical charge.

Stiction in MEMS

For simplicity, consider $F_{\text{ext}} = 0$ in Eq. 1 and find the steady-state (static equilibrium) solutions. Under static equilibrium, Eq. 1 can be transformed to

$$Z = \frac{\beta}{2(1-Z)^2} \qquad (2)$$

where normalized displacement $Z = \frac{Y}{d} (0 \le Z \le 1)$

dimensionless parameter $\beta = \frac{\varepsilon AU^2}{Kd^3}$

Nonlinear algebraic Eq. 2 can be transformed into a cubic equation and solved using Cardano's method.[3] This equation has three real-value solutions if

$$0 \le \beta < \frac{8}{27} \left(\begin{array}{l} \text{or } 0 \le U < U_{\max} \text{ where } U_{\max} \text{ is defined} \\ \text{from the relation } \frac{\varepsilon AU_{\max}^2}{Kd^3} = \frac{8}{27} \end{array} \right)$$

The parameter $U_{\max}$ is called the pull-in voltage. However, one of the solutions (in the interval $Z > 1$) is clearly unphysical. As is shown below, one of the two physical solutions ($1/3 \le Z \le 1$) is unstable and only the other ($0 \le Z \le 1/3$) describes the stable steady state. The stable solution of the steady-state Eq. 2 is

$$Z_1 = \frac{2}{3}\left\{ 1 - \cos\left[\frac{1}{3}\arccos\left(1 - 2\left(\frac{U}{U_{\max}}\right)^2 \right) \right] \right\}$$

In the case $U \ge U_{\max}$, Eq. 2 has a single real-value solution that is definitely unphysical (no static equilibrium for the 'weak' spring).

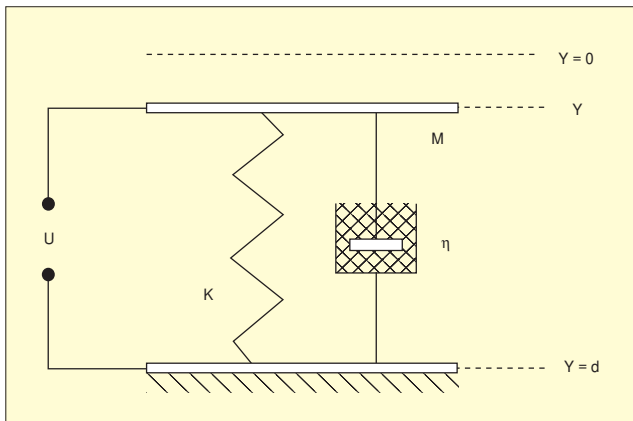The graphical method shown in Figure 2 can clearly explain

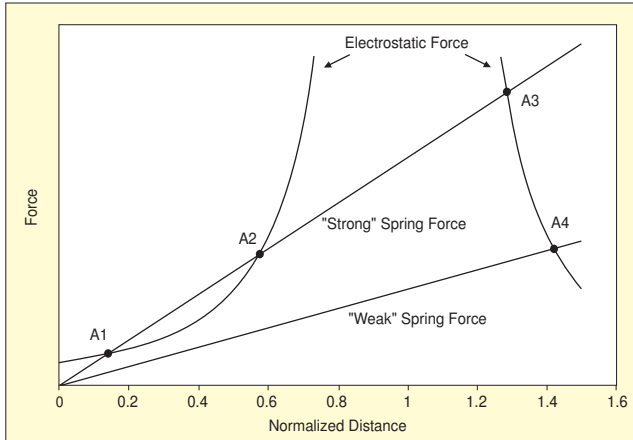Figure 1. Electrostatic parallel-plate model with a moving upper plate.

Figure 2. Diagram illustrating the graphical solution of Eq. 2 and identification of stable and unstable steady-states.
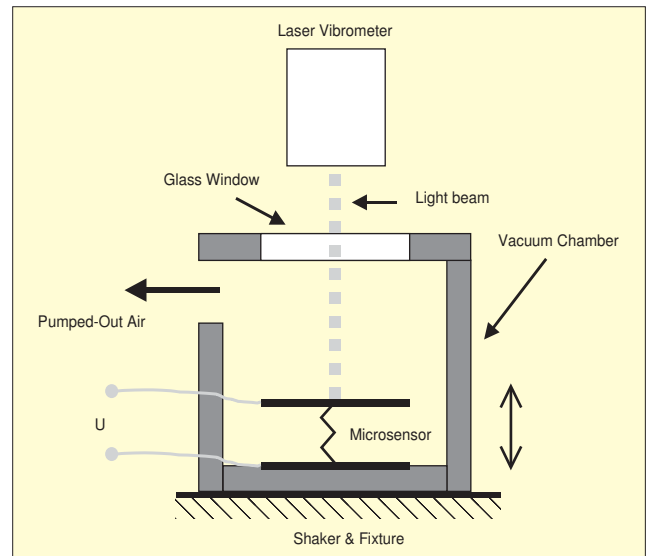

Figure 3. Experimental setup for sweep-sine testing of a capacitive microsensor in a vacuum.
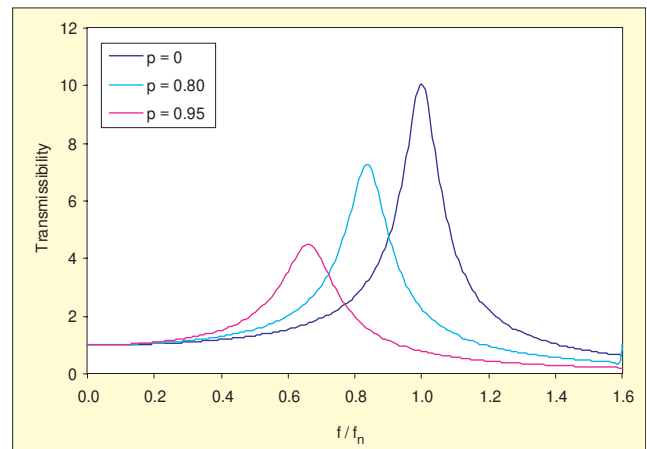

Figure 4. The transmissibility calculated at three voltage levels $p = U/U_{max}$ for hysteresis friction ($\eta = const$); the parameter f_n is the natural frequency at zero voltage ($p = 0$).

why one steady state is stable and the other is unstable. The straight lines represent the dimensionless elastic forces (the left side of Eq. 2) for a 'strong' and 'weak' spring. The parabolic curves signify the dimensionless Coulomb (electrostatic) force (the right side of Eq. 2). The intersection points (A_1, A_2 and A_3 for the 'strong' spring; A_4 for the 'weak' spring) represent all real-value solutions of Eq. 2; the solutions A_3 and A_4 are not physical.

Let's check the solution $Z = Z_1$ (point A_1) for stability. At the interval $0 \le Z \le Z_1$, the electrostatic force exceeds the mechanical spring force and therefore pulls the upper plate toward point A_1; at $Z_1 < Z < Z_2$ ($Z = Z_2$ corresponds to point A_2) the mechanical spring force exceeds the electrostatic force and pushes the upper plate back to point A_1. However at $Z_2 < Z < 1$, the dominating electrostatic force pulls the upper plate from point A_2 to the fixed bottom plate. So, the steady-state position $Z = Z_1$ (point A_1) is stable and the position $Z = Z_2$ (point A_2) is unstable. This instability results in stiction (as the upper plate collides and sticks to the bottom plate), one of the critical failure modes in MEMS. Remember that the stability criterion

$$Z = \frac{Y}{d} < \frac{1}{3} \tag{3}$$

is valid only for static equilibrium (if the upper plate has zero velocity). Otherwise, the mechanical inertia changes the stability zone determined by Eq. 3. However at relatively low frequencies, the inertial force is small in comparison with the elastic force and Eq. 3 is a good approximation. In practice, sporadic stiction events are prevented by spacers made of electrical isolator material and commonly located on the bottom plate; the height of such spacers slightly exceeds $2d/3$.

Negative Spring Effect

The negative spring effect was discovered long ago but is still becoming public knowledge. Some former colleagues had believed it only after the author conducted a few illustrative sweep-sine shaker tests. A small vacuum chamber with the capacitive MEMS transducer inside was fixed in a single-axis shaker (Figure 3). The air was pumped out from the chamber to mitigate the squeeze-film effect, distorting the high-frequency response. The upper plate velocity was measured by a single-point laser-vibrometer through a glass window. The voltage on the capacitive transducer varied from one experiment to the next. The sweep-sine frequency response was calculated as the ratio of the upper plate velocity to the shaker velocity. The experimental results (similar to those shown in Figure 4) clearly indicated that both resonant frequencies and quality factors notably reduce with voltage. The "negative quality factor effect" is explained in the next section.

To theoretically interpret the "negative spring effect," determine the effective spring constant K_{eff} as equal in magnitude but opposite in sign to the space derivative of the combined elastic and electrostatic force:

$$K_{eff} = -\frac{\partial \left[-KY + \dfrac{\varepsilon A U^2}{2[d-Y]^2} \right]}{\partial Y} = K\Psi(Z) \tag{4}$$

where the dimensionless factor

$$\Psi(Z) = \frac{K_{eff}}{K} = 1 - \frac{\beta}{(1-Z)^3} = \frac{1-3Z}{1-Z}, \tag{5}$$

and $Z = Z_1$ is the stable solution of Eq. 2. From Eq. 5 for the

stable steady-state solution ($0 \leq Z \leq 1/3$), factor $\Psi(Z)$ and thus the effective spring constant K_{eff} monotonously reduces with Z from 1 to 0 and from K to 0, respectively. The negative spring effect can be referred to as a softening type of non-elasticity.[3] For numeric evaluation, consider three practical cases: $Z = 0.05$, $Z = 0.1$ and $Z = 0.2$. As follows from Eq. 6, the appropriate effective spring constants are below the mechanical spring constant by 11, 22 and 50%, respectively. The appropriate natural frequency

$$f_{neff} = \frac{1}{2\pi}\sqrt{\frac{K_{eff}}{M}} \qquad (6)$$

would reduce respectively by 5, 12 and 29%. For relatively low loss factors ($\eta << 1$) the resonant (measured) and natural frequency nearly coincide and therefore the above results can be observed experimentally.

Negative Quality Factor Effect

The quality factor Q describes the shape of a resonant frequency response: the higher and narrower the resonant peak, the higher the quality factor. For a 1-DOF vibratory system, the quality factor is inversely proportional to the loss factor. From Eqs. 1 and 4, the magnitude of the dissipative force equals

$$F_{damp} = K\eta Y = K_{eff}\eta_{eff}Y,$$

so, the effective loss factor $\eta_{eff} = \eta/\Psi(Z)$ grows with voltage (because the function $\Psi(Z)$ reduces with voltage). Such a phenomenon has nothing to do with an increase in the energy dissipation. The energy dissipated during one vibration cycle remains the same at each frequency but the ratio of this energy to the system's elastic energy decreases due to the negative spring effect. As a result, the quality factor $Q = 1/\eta_{eff} = \Psi(Z)/\eta$ and hence reduces with voltage.[3] As the resonant frequency also decreases with voltage (due to the negative spring effect), the above result is always valid if the mechanical loss factor is constant or reduces with frequency and is less pronounced in case of viscous friction (with the loss factor linearly growing with frequency). For instance, if the normalized displacement $Z = 0.2$, then factor $\Psi(Z) = 0.5$, so the quality factor decreases by 50% (compared to the zero voltage case) for the frequency-independent loss factor, and by 29% in the case of viscous friction.

Squeeze-Film Damping

In the above discussion, we neglected the potentially high forces in the narrow air film between the plates. Such an approximation is reasonable at relatively low frequencies or under a specific vacuum. However, at high frequencies, the air film effects become dominant. The upper plate's displacement tends to squeeze the air film in and out of the gap. Due to air viscosity, this movement is resisted and results in a pressure gradient in the gas film. The pressure gradient builds the counterforce with two components. One component represents the spring-like behavior of the air and is linear with the upper plate displacement. The other (quadrature) component represents damping and is proportional to the upper plate's velocity. The squeeze-film process can be described by Navier-Stokes momentum equations and continuity equation or by a simplified differential equation called the Reynolds equation.[4,5] We will restrict our consideration only to the damping. If the upper plate moves perpendicular to the bottom plate, the squeeze-film component of the total loss factor is derived as

$$\eta_{squeeze} = \frac{\alpha}{2\pi}\frac{\mu L^4}{M f_{neff} d^3}\frac{f}{f_{neff}} \qquad (7)$$

where:

f = vibration frequency
f_{neff} = effective natural frequency defined by Eq. 6
μ = dynamic viscosity of air ($\approx 1.8 \times 10^{-5}$Pa $\times$ s under atmospheric pressure)
L = horizontal dimension (radius or length/width) of the plates

α = dimensionless coefficient depending on the plates' shape (approx. 0.42 for square plates)

For evaluation, consider that the plates are square with: $L=2$ mm=0.002m; $d=10\mu m=10^{-5}$m; $M=10^{-5}$kg; and $f_{neff}=3000$Hz. Substituting these data into Eq. 7, calculate $\eta_{squeeze} \approx 0.6 \ f/f_{neff}$. So in this particular case, the squeeze-film component of the loss factor does not exceed 0.05 if $f \leq f_{neff}/12 \approx 250$ Hz but increases to 0.6 at $f = f_{neff}$. The squeeze-film effect is mitigated by increasing the gap, reducing the horizontal size, making holes in the plates and (best of all) by reducing air pressure in the gap. The latter is feasible for the following reason. In the macro world air viscosity just slightly depends on air pressure, but in micro systems the situation is quite different because the mean free molecular path can become smaller than the air gap even due to a feasible reduction of the air pressure and therefore the air flow can't be treated as a continuum (with the collisions occurring mainly between air molecules), and molecular slip flow occurs. At slip flow, the air molecules strike the plates rather than other air molecules. Thus, their interaction at the micro level (resulting in the viscous friction in the micro world) becomes insignificant.

Gravity Effect

If a capacitive sensor continuously remains at the same position and orientation, the upper plate displacement caused by gravity is constant and can be balanced out by calibration. The variation of the position is not of great concern unless the device belongs to a space vehicle. However, the change in the orientation may be vital. Consider two similar but oppositely directed capacitive microsensors (Figure 5). One of the transducers is oriented like our conventional model, the other is rotated through 180°. In the first case, the movable plate shifted by the gravity reduces the air gap. In the second case, the gravity increases the gap between the plates. So, the displacements caused by the gravity force are equal in magnitude and opposite in sign. Each displacement's magnitude Y_g is calculated from simple equation $Mg = K_{eff}Y_g$ (here g $\approx$ 9.81 m/s^2 is acceleration of gravity). Taking into account Eq. 6, we obtain

$$Y_g = \frac{Mg}{K_{eff}} = \frac{g}{(2\pi f_{eff})^2}. \qquad (8)$$

So, the displacement magnitude can be predicted using Eq. 8 and the resonant frequency f_{eff} measured on sweep-sine shaker test. In particular for $f_{eff} = 2000$ Hz, the displacement

$$Y_g \approx \frac{9.81}{(2\pi 2000)^2}\text{ m} \approx 0.06 \ \mu\text{m}.$$

This value is indeed not minor. For a gap thickness of 6 μm, Eq. 3 calculates the stable steady-state zone to be under 2 μm, so the practical operative range seems not likely to exceed 1.2 μm. Thus, the displacement caused by gravity covers 0.06 / 1.2 = 5% of the operative range. In this case for an individual sensor, the relative error inflicted by gravity under a variable orientation can cover 10% of the operative range. How to compensate such a notable error? Eq. 8 indicates that the error decreases with the resonant frequency: if the resonant frequency could be changed to 10,000 Hz, the error would reduce to

$$\left(\frac{2,000}{10,000}\right)^2 10\% = 0.4\%$$

of the operative range. Another simple but effective solution is to apply the array of two closely-spaced, similar but oppositely directed capacitive transducers (as shown in Figure 5) and average two signals. For example, if the transducers measure static or sound pressure, they produce electric signals $Y_1 = A - B$ and $Y_2 = A + B$ where component A describes the measured pressure and component B is the error imposed by the gravity force. The average value
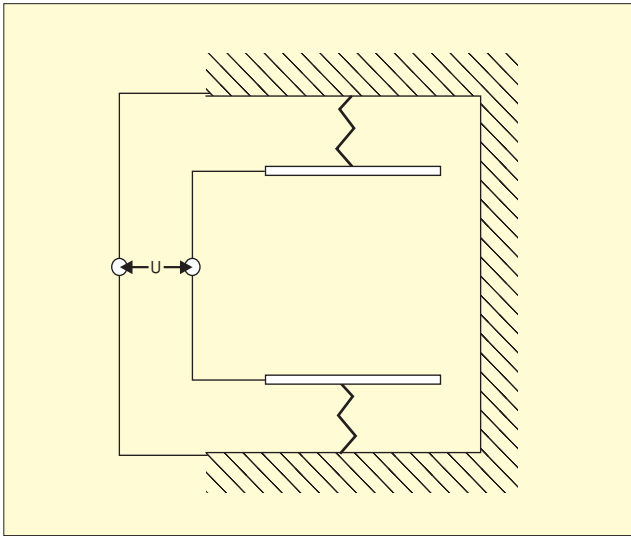
$$Y_{av} = \frac{Y_1 + Y_2}{2} = A$$

Figure 5. Array of two similar but oppositely directed microsensors.

and the systematic error caused by gravity decays to zero. Although even analogous devices are not exactly identical, the error can still remain negligible. It is important that such an array-based design works with its axis tilted at any arbitrary angle.

Mitigation of Environmental Effects

Ambient vibration and acoustic noise are of special attention because occasionally they 'kill' otherwise promising MEMS designs. The remedies exist but they are not readily feasible. Traditional spring vibration isolators are effective only well above their own resonant frequencies. As the total mass of a common MEMS package is relatively low, the stiffness of the elastic mountings should be very limited to design a reliable passive isolation system. In case of low operational frequencies, an active vibration control system should be incorporated into the MEMS package design. The optional passive solution is based on the same compensation principle as for gravity effect mitigation (Figure 5). It is noteworthy that MEMS vibration caused by impacts or transient effects mostly occurs at the resonant frequencies of the MEMS elements. In this case, squeeze-film damping can be utilized for attenuation but only if the MEMS transducer does not operate under a vacuum. Error compensation through signal processing (based on frequency modulation, etc.) is effective if the operational frequency is beyond the noise frequency range. It should be assumed that the creation of an effective vibration and sound isolation system for MEMS designs requires specific skills, experience and techniques.

Helmholtz Resonance

Not long ago, the author experimentally studied a miniature model of a 'room' incorporating a ceramic 'floor' and "side walls" (each 1 mm thick) with two rectangular ($\approx 0.5 \times 4$ mm^2) slots. The MEMS element playing the role of the 'ceiling' consisted of a small silicon disc (3 mm in diameter and 0.5 mm thick) and a circular rubber membrane in the rectangular silicon frame (Figure 6). The 'room' was installed in a 1-DOF shaker for sweep sine testing, the disk vibration was measured with a single-point laser-vibrometer. The transmissibility (the ratio of the amplitudes of the disk and shaker velocities) proved to contain two peaks (Figure 7). At 2000 Hz, one was related to the disk-membrane resonance and the other (at 3500 Hz) was identified as a Helmholtz resonance. The simplest Helmholtz resonator is a container of gas (usually air) with a small hole or open neck[6] (like an empty bottle). At low frequencies (if the acoustic wavelength notably exceeds the resonator's dimensions), the air in and near the neck moves like a solid mass compressing or expanding a spring (the air volume). If the air volume is V, the circular hole or flanged cylindrical neck has cross-sectional area S, and the speed of sound in air is $c \approx 340$
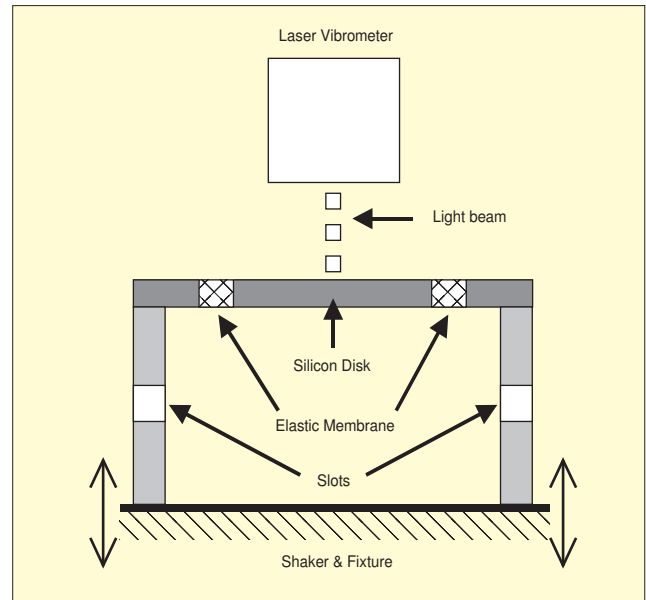

Figure 6. Experimental vibration setup for sweep-sine shaker testing of a miniature silicon disk on an elastic membrane.
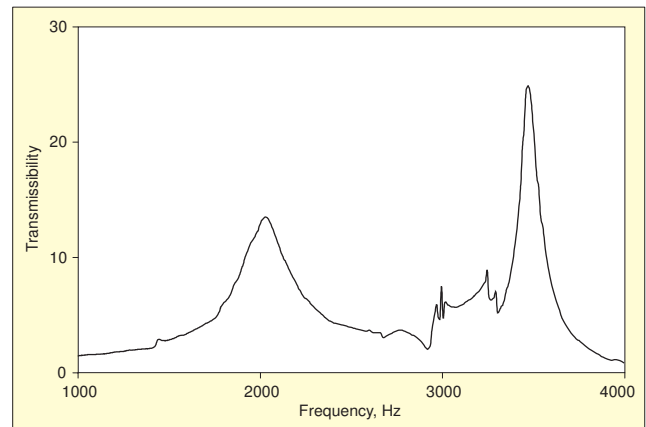

Figure 7. Vibration transmissibility measured on a disk; the higher peak indicates a Helmholtz resonance.

m/s, the Helmholtz resonant frequency is given by the equation

$$f_H \approx \frac{c}{2\pi} \sqrt{\frac{S}{V\left(h + 0.8\sqrt{S}\right)}} \qquad (9)$$

where h is the neck length or (in case of a hole) the wall thickness.[6]

As seen from Figure 7, the Helmholtz resonance peak transmissibility was rather high (about 25). The author originally designed that experiment for vibration fatigue testing on the MEMS element but as he observed the model, he realized that it can also be used to simulate one of the effects of environmental vibration in residential dwellings. In this particular case, the physics of micro and macro models are similar. For instance, a dwelling room can operate at very low frequencies like a Helmholtz resonator where the open window functions as a hole. For a rectangular room with the volume 5 m × 3 m × 3 m = 45 m^3, wall thickness $h = 0.1$ m, and open window modeled for simplicity as a round hole with the radius 0.5 m, Eq. 9 gives $f_H \approx 8$ Hz (an infrasonic frequency). There are many case stories on the low-frequency 'hum' that is not perceived by the majority of people but upsets about 2% of residents at their homes with headaches, nausea, fatigue and joint pain.[7] In Kokomo, IN, a strong component of infrasound around 10 Hz was measured inside some dwellings on a survey sponsored by Fox TV.[8] Such a 'hum' can be initiated by environmental vibration or acoustic noise at infrasonic frequencies and magnified due to the Helmholtz resonance.[9] It is costly and time

consuming to simulate the effect of environmental vibration on real-scale models but micro models can save money and time.

Conclusions

The main vibroacoustic effects in capacitive (electrostatic) MEMS were introduced to engineers engaged in high-technology projects. The scope is important because vibration problems have often 'killed' promising designs and even whole companies. The challenges prove knotty because some micro world phenomena are unusual to the macro world. The physical interpretation was done through simplified theoretical models and feasible experimental results. Hopefully this article will help in developing and testing electrostatic microtransducers, but some results may also support other high-tech applications.

References

1. Hunt, F. V., *Electroacoustics*, Acoustical Society of America. 1954.
2. Nathanson, H. C., Newell, W. E., Wickstrom, R. A., and Davis, J. R., "The Resonant Gate Transistor," IEEE Tran. On Elec. Dev., 14 (3), 117-133, 1967.
3. Vinokur, R. Y., "Feasible Analytical Solutions for Electrostatic Parallel-Plate Actuator or Sensor," *Journal of Vibration and Control*, to be published in 2003.
4. Langlois, W. E., "Isothermal Squeeze Films," *Quarterly Applied Mathematics*, 20 (2), 131-150, 1962.
5. Blech, J. J., "On Isothermal Squeeze Films," *Journal of Lubrication Technology*, 105 (Oct), 615-620, 1983.
6. Morse, P. M., *Vibration and Sound*, Acoustical Society of America, USA, 1981.
7. Krylov, V. V., "Investigation of Environmental Low-Frequency Noise," *Applied Acoustics*, 51(1), pp. 33-51, 1997.
8. "The 'Hum' is Back," *Echoes* (edited by T. Rossing), 12 (3), p.5, 2002.
9. Vinokur, R. Y., "Infrasonic Sound Pressure in Dwellings at the Helmholtz Resonance Actuated by Environmental Noise and Vibration," *Applied Acoustics*, to be published in 2003. **SV**

The author can be reached at: rvinokr@aol.com.